

On the Multiplicity Distributions of Charged Secondaries in the Collisions of Relativistic Nuclei

S.M. ESAKIA¹, V.R. GARSEVANISHVILI^{2,3}, T.R. JALAGANIA⁴
G.O. KURATASHVILI¹, YU.V. TEVZADZE¹

- ¹ Institute of High Energy Physics, Tbilisi
State University, 380086 Tbilisi, Rep. of Georgia
E-mail: tevza@sun20.hepi.edu.ge
- ² Laboratoire de Physique Corpusculaire,
Université Blaise Pascal, 63177 Aubière Cedex France
E-mail: garse@clrvax.in2p3.fr
- ³ Mathematical Institute of the Georgian Academy of Sciences,
380093 Tbilisi, Rep. of Georgia
E-mail: garse@imath.acnet.ge
- ⁴ Department of Physics, Tbilisi State University,
380000 Tbilisi, Rep. of Georgia
Contact author: Yu. V. Tevzadze
E-mail: tevza@sun20.hepi.edu.ge

Abstract

Multiplicities of charged secondary hadrons in the relativistic nucleus–nucleus collisions in a wide energy range are analysed on the basis of partial stimulating emission and cluster cascading models. The experimental data are obtained by means of the two metre propane bubble chamber of JINR (Dubna). The results are compared with the corresponding data for pp and $\bar{p}p$ -collisions at higher energies. It is shown that the regularities in pp and $\bar{p}p$ -interactions at high energies and wide energy range and in nucleus-nucleus interactions at relatively low energies per nucleon and narrower energy range are similar.

Key words: relativistic heavy ions, multiplicity distribution, partial stimulating, cluster cascading.

1 Introduction and Basic Notions

The interest to the study of multiplicity distributions of charged secondaries has been increased again after the new powerful accelerators have been constructed and the beams of protons, antiprotons, electrons, positrons and heavy ions have been obtained (see,e.g. [1-5]).

In the present work multiplicities of charged secondary hadrons in pp , $\bar{p}p$ and nucleus-nucleus collisions in a wide energy range are analysed on the basis of partial stimulating emission (PSE) and cluster cascading models (CCM). The manifestation of the negative binomial distribution (Pascal distribution)

$$P_n = \frac{(n+k-1)!}{(k-1)!n!} \left(\frac{\langle n \rangle}{\langle n \rangle + k} \right)^n \left(\frac{k}{\langle n \rangle + k} \right)^k \quad (1)$$

in the multiplicity distributions of secondaries is interpreted in the framework of these models.

In Eq.(1) $\langle n \rangle = \langle n_{\pm} \rangle$ is the average multiplicity of all charged secondaries. Parameter k determines the form of the distribution, e.g. if $k^{-1} = 1$ we get the geometrical distribution, if $k^{-1} = 0$ we get the Poisson distribution.

It is useful to establish a recurrence relation between P_n and P_{n+1} [6]. When deriving this relation one starts from the consideration that the event with multiplicity $(n+1)$ can be expressed by means of $(n+1)$ number of events with multiplicity n :

$$g(n) = \frac{(n+1)P_{n+1}}{P_n} \quad (2)$$

Inserting Eq.(1) into Eq.(2) one can express $g(n)$ as:

$$g(n) = a + bn, \quad (3)$$

where:

$$a = \frac{k \langle n \rangle}{k + \langle n \rangle}, \quad b = \frac{\langle n \rangle}{k + \langle n \rangle} \quad (4)$$

From here one can write:

$$\langle n \rangle = \frac{a}{1-b}, \quad k = \frac{a}{b} \quad (5)$$

Dispersion $D = (\langle n^2 \rangle - \langle n \rangle^2)^{1/2}$ of the distribution (1) and parameters $\langle n \rangle$ and k are related as:

$$k = \frac{\langle n \rangle^2}{D^2 - \langle n \rangle} \quad (6)$$

PSE model admits the following interpretation of the distribution (1) and the relation (3) [6]. The emitted particles are uniformly distributed among k cells. These cells do not correlate and there is no connection between the particles in different cells. The additional $(n + 1)$ -th particle can be emitted in the initial act of the collision independently of the already existing n particles. This is reflected by the constant term α in the function $g(n)$. In this case $b = 0$ (i.e. $k^{-1} = 0$) and the classical Poisson distribution is obtained. But such an emission can be intensified as a result of quantum interference effects. The average effect of this intensification is expressed by adding the linear term bn ($b = \text{const}$) in the function $g(n)$. It follows from the Eqs. (3) and (5) that:

$$g(n) = a \left(1 + \frac{n}{k} \right) \quad (7)$$

One can conclude that n/k is the average number of particles among already existing n particles which promote the creation of a new $(n + 1)$ -th particle. So k^{-1} is the relative average fraction of particles which stimulate such creation.

On the other hand the multiple production can be interpreted in the framework of CCM. One assumes here that after the collision of high energy particles (leptons, hadrons, nuclei) some excited n -particle system is produced which is formed as an N -cluster state. Each of these clusters is formed by the particles which are produced directly or indirectly from one particle produced in the initial act of the collision. These latter particles are called the "patriarchs" of the clusters. The "patriarch" which does not produce secondaries forms one particle cluster itself. It is assumed that "patriarchs" and consequently clusters are produced independently from each other. Therefore for the multiplicity of clusters the Poisson distribution holds:

$$F(N) \sim \frac{1}{N!} \langle N \rangle^N \quad (8)$$

For the better understanding of the CCM let us give a short review of the formulae of this model. It is evident that the average number of clusters $\langle N \rangle$ is given by the formula:

$$\langle N \rangle = \frac{\langle n \rangle}{\langle n_c \rangle} \quad (9)$$

where $\langle n \rangle$ is the average number of charged hadrons, $\langle n_c \rangle$ is the average number of hadrons in the cluster.

Let $F_c(n_c)$ be the distribution of particles inside one cluster. It is assumed in the CCM that the recurrence relation between $F_c(n_c + 1)$ and $F_c(n_c)$ is of the form:

$$g_c(n_c) = \frac{(n_c + 1)F_c(n_c + 1)}{F_c(n_c)} = bn_c, \quad b = \text{const}, \quad n \geq 1 \quad (10)$$

The meaning of this relation is that the effect of the creation of $(n_c + 1)$ -th particle is proportional to the number of particles already existing in the cluster in average. Iterating Eq.(10) one gets:

$$F_c(n_c) = F_c(1) \frac{b^{n_c-1}}{n_c} \quad (11)$$

where $F_c(1)$ can be found from the normalization condition:

$$\sum_{n_c} F_c(n_c) = 1 \quad (12)$$

From here one gets:

$$F_c(1) = -\frac{b}{\ln(1-b)} \quad (13)$$

One can find the following average values:

$$\langle n_c \rangle = \sum_{n_c} n_c F_c(n_c) = \frac{F_c(1)}{1-b} \quad (14)$$

$$\langle n_c^2 \rangle = \sum_{n_c} n_c^2 F_c(n_c) = \frac{\langle n_c \rangle}{1-b} \quad (15)$$

Note finally that on the basis of Eqs.(8) and (11) one can write the expression for the total multiplicity n in the form of the negative binomial distribution which is represented in the form [6]:

$$P_n \sim a(a+b)[a+b(n-1)] \quad (16)$$

where

$$a = \langle N \rangle F_c(1) \quad (17)$$

Inserting Eq.(16) into the recurrence relation (2) one gets again Eq.(3). The identification of the parameters a and b which is given by Eqs.(10) and (17) completely corresponds to their earlier physical meaning. So the CCM is compatible with the negative binomial distribution.

2 Analysis of the Experimental Data

The experimental data are obtained on the two-metre propane bubble chamber (PBC-500) of the Laboratory of High Energies of JINR (Dubna) with tantal targets in it which were bombarded by p , d , He and C beams[5]. The data on pp (ISR and others) and $\bar{p}p$ (UA5- Collaboration) collisions in a wide energy range [1-4,6] are used for comparison.

It was shown in Ref.[4] that in pp and $\bar{p}p$ - collisions ($10 \leq \sqrt{s} \leq 900 GeV$) k^{-1} increases linearly and reaches the value 0.31 at $\sqrt{s} = 900 GeV$, i.e. every third particle is actively interacting. The average number of charged particles in the cluster $\langle n_c \rangle$ reaches the value 4.55, the average number of clusters reaches the value 8. May be there is even a decrease of the number of clusters as compared to the energy $\sqrt{s} = 540 GeV$ (Table 1). The width of the distribution of charged particles in the clusters increases with increasing energy much faster than the corresponding dependence for the total multiplicity. The ratio $R = \langle n \rangle / D^2$ decreases 12 times in the range $8.33 \leq \sqrt{s} \leq 900 GeV$. The same quantity for the clusters $R_c = \langle n_c \rangle / D_c^2$ decreases 400 times (Tables 1a and 1b, Fig. 1). Such a decrease is observed up to $\sqrt{s} = 200 GeV$ and after that R and R_c behave almost in the same way. After $\sqrt{s} = 200 GeV$ a tendency of the narrowing of the multiplicity distributions in the cluster and the total multiplicity is observed.

What is the behaviour of $R = f(E)$ and $R_c = f(E)$ for pTa -collisions in the range 2-10 GeV? A fast decrease of R and especially of R_c is observed up to the energy 5 GeV, i.e. the dispersion increases fast (Table 2, Fig. 2) At the energies higher than 5 GeV a change of the regime is observed and probably they behave as constants. The constant regime in pp and $\bar{p}p$ -collisions is observed from $\sqrt{s} = 200 GeV$.

Consider the same dependences for dTa , $HeTa$ and CTa -collisions (Tables 3,4,5). For dTa -collisions $R_c(E)$ decreases faster than $R(E)$. The situ-

ation is the same as in pTa -collisions in the same energy range. In the case of $HeTa$ and CTa -collisions the behaviours of $R_c(E)$ and $R(E)$ are similar.

It is interesting to note that a similar picture arises, if we consider the dependence of R and R_c on the atomic weight A_i of the projectile nucleus. For pTa , dTa , $HeTa$ and CTa -collisions at 4.2 AGeV R and R_c decrease with increasing A_i . But, if R decreases 19 times, R_c decreases 50 times. Further, the ratio R_c/R is approximately equal to 8 for pTa -collisions and is equal to 1.5 for CTa -collisions at the same energy, i.e. this ratio tends to one with increasing A_i .

In Ref.[7] the dependence $k^{-1} = f(s)$ for pp and $\bar{p}p$ -collisions in the range $10 \leq \sqrt{s} \leq 900\text{GeV}$ is approximated by the formula:

$$k^{-1} = a_1 + b_1 \ln \sqrt{s} , \quad (18)$$

$k^{-1} > 0$ and decreases rather slowly with increasing energy ($b_1 \approx 0.06$). It has been shown by our analysis that at lower energies, in particular, at $\sqrt{s} < 8.33\text{GeV}$ (corresponding laboratory energy is 36 GeV) $k^{-1} < 0$. At higher energies k^{-1} becomes positive.

Consider now nucleus-nucleus collisions. If by analogy with Eq.(18) we approximate k^{-1} by the formula:

$$k^{-1} = a_2 + b_2 \ln E, \quad (19)$$

it turns out that in a narrow energy range (2-5 GeV) a fast increase of k^{-1} is observed, $b_2 \geq 0.15$ (Tables 3,4,5, Fig. 3). For the energies higher than 5 GeV the fast increase of k^{-1} is slowed down. The essential feature of pTa -collisions is that at the energy 2.48 GeV the parameter k^{-1} becomes negative. Starting from 4.3 GeV (may be earlier) k^{-1} becomes positive, i.e. there is a similarity with pp - collisions but at lower energies. For dTa , $HeTa$, CTa -collisions parameter k^{-1} is positive and increasing with increasing energy, i.e. the growth of the atomic weight of the incoming nucleus plays the same role as the growth of energy in pp -collisions (Tables 1, 3-5, Refs.[1-8]).

Consider the situation with negative k^{-1} in some detail. Note that one writes nothing about them in Ref.[6], though they are obtained from the experimental data (Tables 1a,2, Refs.[9,10]). Probably the reason is that the negative binomial distribution and PSE and CCM in their strict formulations assume the positiveness of k^{-1} . But the stable presence of negative k^{-1} made us to take a broader view to this problem. First of all, if we consider the

negative binomial distribution in the form of Eq.(16) and compare it with the Polya-Egenberger distribution (see, e.g. [10])

$$P_n = \left(\frac{\langle n \rangle}{1 + g^2 \langle n \rangle} \right)^n \left(\frac{1}{1 + g^2 \langle n \rangle} \right)^{1/g^2} \frac{1}{n!} \sum_{\alpha=0}^{n-1} (1 + \alpha g^2), \quad (20)$$

where $g^2 = (D^2 - \langle n \rangle) / \langle n \rangle^2$, it is evident that these two distributions coincide. The role of the parameter $k^{-1} = b/a$ is played by g^2 . But the sign of the parameter g^2 in the Eq.(20) is not fixed. In particular, if $g^2 = 0$, we get the Poisson distribution, if $g^2 > 0$, this distribution is broader than the Poisson one, if $g^2 < 0$, it is narrower than the Poisson one. So parameter g^2 can be thought as a measure of deviation of the distribution from the Poisson one and if we perform the analysis of the experimental data in terms of the Polya-Egenberger distribution, parameter $k^{-1} = g^2$ can take positive and negative values as well. Further, there are some grounds to think that the negative values of k^{-1} are compatible with the assumptions of PSE and CCM. In fact, the second term in Eq.(3) corresponds to quantum-mechanical interference effects. If this effects stimulate the creation of $(n+1)$ -th particle, then $b > 0$ and hence $k^{-1} = b/a > 0$, since $a > 0$. But it is natural to suppose that this effects can make weaker the emission (capture of the particle). In this case $\beta < 0$ and hence $k^{-1} < 0$. So one can conclude that $k^{-1} < 0$ corresponds to the capture of secondary particles (see also [5,11]).

Proceed now to consider the energy dependence of the total average multiplicity of particles $\langle n \rangle$ and the average multiplicity of particles in the clusters $\langle n_c \rangle$ in $A_i T a$ -collisions and compare this data with corresponding results on pp and $\bar{p}p$ -collisions. In the energy range 7.42-200 GeV in pp and $\bar{p}p$ - collisions $\langle n \rangle$ and $\langle n_c \rangle$ increase rather fast, but $\langle n \rangle$ increases faster than $\langle n_c \rangle$. In the range (200-900) GeV the increase of these quantities is slower and both of them increase 1.6 times (Table 1).

Consider now $pT a$, $dT a$, $HeT a$ and $CT a$ -collisions. In $pT a$ - collisions the energy range can also be divided into two parts. The first interval (2-5) GeV and the second one (5-9) GeV. In the first interval we observe a more rapid increase of the average multiplicities $\langle n \rangle$ and $\langle n_c \rangle$ than in the second one (Table 3, Fig. 4). So we have qualitatively the same situation as in pp and $\bar{p}p$ - collisions, but the energy range is more narrow and low. In $dT a$, $HeT a$ and $CT a$ -collisions in the energy range (2-5) GeV the average multiplicities $\langle n \rangle$ and $\langle n_c \rangle$ increase similarly with increasing energy.

It is interesting to trace the dependence of $\langle n \rangle$ and $\langle n_c \rangle$ on the atomic weight A_i of the incoming nucleus at fixed energy. It is seen from Tables 3,4,5 and Fig. 4 that at 2.5 GeV $\langle n_c \rangle$ increases 3 times and at 4.3 GeV - 4 times. The behaviour of $\langle n \rangle$ is similar. So the increase of the atomic weight of the incoming nucleus in $A_i A_t$ -collisions plays a similar role as the increase of the energy. As a result in $A_i A_t$ -collisions the same effect is achieved at relatively low energies as compared to hadron- hadron collisions. This can be confirmed by the following example: in CTa -collisions at 2.48 AGeV $\langle n_c \rangle = 2.66$ and at 4.30 AGeV $\langle n_c \rangle = 4.55$. The same number of particles is contained in the clusters in $\bar{p}p$ -collisions at $\sqrt{s} = 200\text{GeV}$ and $\sqrt{s} = 900\text{GeV}$, respectively.

It is interesting to study the dependences of the dispersions on $\langle n \rangle$ and $\langle n_c \rangle$:

$$D = f(\langle n \rangle), \quad (21)$$

$$D_c = f(\langle n_c \rangle) \quad (22)$$

It is seen from Fig. 5 that at the energies higher than 5 GeV the data for the dependence (21) for hadron-hadron and nucleus-nucleus collisions lie on two different curves (curves 1 and 2), but the data for the dependence (22) lie on the same curve (curve 3).

Let us show in conclusion the multiplicity distribution of charged secondaries in dTa -collisions at 5.18 AGeV and its fit according to Eq.(1) (Fig. 6) with only normalization parameter, which is approximately equal to one, $\chi^2/N = 1.15$, N is the number of experimental points.

The authors are indebted to the staff of two metre propane bubble chamber of JINR (Dubna) for supplying the data. They would like to thank Ya. Darbaidze, E. Khmaladze, N. Kostanashvili, P. Pras, G. Roche, T. Topuria, M. Topuridze for interesting discussions. On of the authors (V.R.G.) expresses his deep gratitude to Bernard Michel and Guy Roche for the warm hospitality at the Laboratoire de Physique Corpusculaire, Université Blaise Pascal, Clermont-Ferrand, to V. Kadyshesky, T. Kopaleishvili, H. Leutwyler, W. Rühl for supporting his stay at the L.P.C. and to NATO for supporting this work.

3 References

1. A.Breakstone et al. *Phys.Rev.*, 1984, v.D30, p.528
2. G.J.Alners et al. *Phys. Lett.*, 1984, v.B138,p.304 R.Ansorge et al. *Charge Particle Multiplicity Distributions at 200 and 900 GeV c.m.energy*,UA5-Collaboration, CERN-EP/88-172
3. M.Althoff et al. TASSO-Collaboration, *Z.Phys.*, 1984 v.C22, p.307
4. G.J.Alners et al. *Phys.lett.*, 1985, v.B160, p.199
5. E.O.Abdurakhmanov et al. *Sov. J. Nucl. Phys.*, 1978, v.27, p.1020; 1978, v.28, p.1304 M.A.Dasaeva et al. *Sov. J. Nucl. Phys.*, 1984, v.39, p.846
6. A.Giovannini, L.Van Hove. *Negative Binomial Distribution in High Energy Hadron Collisions*. CERN-TH 4230/85
7. G.J.Alners et al. *Scaling Violations in Multiplicity Distributions at 200 and 900 GeV*. CERN-EP/85-197; *Phys.Lett.*, 1986, v.B167, p.476
8. V.V.Ammosov et al. *Phys.Lett.*, 1972, v.B42, p.519 D.B.Smith et al. *Phys.Rev.Lett.*, v.B42, p.519
9. N.K.Kutsidi, Yu.V.Tevzadze. *Sov. J. Nucl. Phys.*,1985, v.41, p.236
- 10.C.Vokal, M.Shumbera. *JINR-Communications*, 1-82-388, Dubna, 1982
- 11.N.S.Grigalashvili et al. *Sov. J. Nucl. Phys.*, 1988, v.48, p. 476

TABLE 1A
 Characteristics of the Multiplicity Distributions of Charged Hadrons
 in pp -collisions

	Energy in the c.m.s. \sqrt{s} , GeV				
	7.42	8.33	9.78	30.4	62.2
$\langle n \rangle$	4.56 ± 0.04	4.78 ± 0.03	5.32 ± 0.13	10.7	13.6
D	2.09 ± 0.04	2.23 ± 0.03	2.58 ± 0.05	4.59	6.01
$\langle n \rangle / D^2$	1.04 ± 0.02	0.96 ± 0.04	0.80 ± 0.03	0.51	0.38
k^{-1}	-0.009	0.008	0.05	0.09	0.12
b	-0.044	0.039	0.20	0.49	0.62
$\langle n_c \rangle$	0.98	1.02	1.12	1.43	1.69
D_c	-	0.14	0.38	0.87	1.26
$\langle n_c \rangle / D_c^2$	-	51	7.76	1.88	1.06
$\langle n \rangle / k$	-0.04	0.04	0.25	0.97	1.66
$\langle N \rangle$	4.66	4.69	4.75	7.48	8.05

TABLE 1B
 Characteristics of the Multiplicity Distributions of Charged Hadrons
 in $\bar{p}p$ -collisions

	Energy in the c.m.s. \sqrt{s} , GeV		
	200	546	900
$\langle n \rangle$	21.3 ± 0.80	29.1 ± 0.9	34.6 ± 1.2
D	10.9 ± 0.4	16.3 ± 0.4	20.7 ± 0.6
$\langle n \rangle / D^2$	0.18 ± 0.02	0.11 ± 0.01	0.08 ± 0.01
k^{-1}	0.22	0.27	0.31
b	0.82	0.88	0.92
$\langle n_c \rangle$	2.65	3.46	4.55
D_c	2.77	4.11	6.01
$\langle n_c \rangle / D_c^2$	0.34	0.20	0.12
$\langle n \rangle / k$	4.65	7.88	10.31
$\langle N \rangle$	8.07	8.41	7.60

TABLE 2
 Characteristics of the Multiplicity Distributions of Charged Hadrons
 in pTa -collisions

	Energy per nucleon in the lab. system, GeV			
	2.48	4.30	5.48	9.94
$\langle n \rangle$	2.98 ± 0.06	4.73 ± 0.07	6.12 ± 0.09	7.84 ± 0.13
$\langle n \rangle / D^2$	1.38 ± 0.05	0.74 ± 0.05	0.53 ± 0.05	0.30 ± 0.03
k^{-1}	-0.08 ± 0.01	0.07 ± 0.01	0.15 ± 0.01	0.31 ± 0.02
b	-0.30	0.26	0.47	0.71
$\langle n_c \rangle$	0.86 ± 0.04	1.18 ± 0.05	1.41 ± 0.09	1.97 ± 0.12
$\langle n \rangle / k$	-0.27	0.34	0.91	2.40
D_c	-	0.45	0.82	1.71
$\langle n_c \rangle / D_c^2$	-	5.83	2.08	1.47
$\langle N \rangle$	3.47 ± 0.18	4.01 ± 0.21	4.34 ± 0.22	4.22 ± 0.23

TABLE 3
 Characteristics of the Multiplicity Distributions of Charged Hadrons
 in dTa -collisions

	Energy per nucleon in the lab. system, GeV		
	2.48	4.30	5.18
$\langle n \rangle$	4.46 ± 0.07	7.15 ± 0.10	7.68 ± 0.21
$\langle n \rangle / D^2$	0.68 ± 0.03	0.40 ± 0.05	0.31 ± 0.03
k^{-1}	0.09 ± 0.01	0.22 ± 0.01	0.29 ± 0.03
b	0.29	0.61	0.69
$\langle n_c \rangle$	1.20 ± 0.06	1.65 ± 0.09	1.90 ± 0.12
$\langle n \rangle / k$	0.40	1.57	2.23
D_c	0.50	1.23	1.59
$\langle n_c \rangle / D_c^2$	4.80	1.09	0.75
$\langle N \rangle$	3.72 ± 0.20	4.22 ± 0.22	4.04 ± 0.25

TABLE 4
 Characteristics of the Multiplicity Distributions of Charged Hadrons
 in *HeTa*-collisions

	Energy per nucleon in the lab. system, GeV		
	2.48	4.30	5.18
$\langle n \rangle$	7.64 ± 0.14	10.81 ± 0.15	11.79 ± 0.25
$\langle n \rangle / D^2$	0.42 ± 0.03	0.21 ± 0.02	0.16 ± 0.02
k^{-1}	0.22 ± 0.02	0.35 ± 0.03	0.45 ± 0.05
b	0.61	0.79	0.84
$\langle n_c \rangle$	1.67 ± 0.08	2.41 ± 0.10	2.88 ± 0.16
$\langle n \rangle / k$	1.56	3.76	5.33
D_c	1.22	2.38	3.12
$\langle n_c \rangle / D_c^2$	0.89	0.42	0.29
$\langle N \rangle$	4.19 ± 0.14	4.48 ± 0.23	4.09 ± 0.22

TABLE 5
 Characteristics of the Multiplicity Distributions of Charged Hadrons
 in *CTa*-collisions

	Energy per nucleon in the lab. system, GeV	
	2.48	4.30
$\langle n \rangle$	12.73 ± 0.61	19.75 ± 0.39
$\langle n \rangle / D^2$	0.18 ± 0.02	0.08 ± 0.01
k^{-1}	0.36 ± 0.05	0.56 ± 0.04
b	0.82	0.92
$\langle n_c \rangle$	2.66 ± 0.10	4.55 ± 0.12
$\langle n \rangle / k$	4.66	11.03
D_c	2.78	6
$\langle n_c \rangle / D_c^2$	0.35	0.12
$\langle N \rangle$	4.77 ± 0.22	4.29 ± 0.24

4 Figure Captions

Fig.1 Energy dependence of R and R_c in pp - and $\bar{p}p$ -collisions. $+$ for R , \bullet for R_c .

Fig.2 Energy dependence of R in $pTa(\bullet)$, $dTa(\blacktriangledown)$, $HeTa(\blacksquare)$, $CTa(\blacktriangle)$ -collisions and R_c in $pTa(\circ)$, $dTa(\nabla)$, $HeTa(\square)$, $CTa(\triangle)$ -collisions.

Fig.3 Energy dependence of the parameter k^{-1} in A_iTa - collisions. $pTa(\bullet)$, $dTa(\circ)$, $HeTa(+)$, $CTa(\nabla)$.

Fig.4 Energy dependence of $\langle n \rangle$ in A_iTa - collisions, $pTa(+)$, $dTa(\triangle)$, $HeTa(\square)$, $CTa(\nabla)$.

Energy dependence of $\langle n_c \rangle$ in A_iTa - collisions, $pTa(\bullet)$, $dTa(\blacktriangle)$, $HeTa(\blacksquare)$, $CTa(\blacktriangledown)$.

Fig.5 Dependence $D(\langle n \rangle)$ in e^+e^- , $\bar{p}p$, pp , A_iTa - collisions, $e^+e^-(\times)$, $\bar{p}p$, $pp(\bullet)$, $pTa(\triangle)$, $dTa(\nabla)$, $HeTa(\blacktriangledown)$, $CTa(\blacktriangle)$, curves 1 and 2.

Dependence $D_c(\langle n_c \rangle)$, in e^+e^- , $\bar{p}p$, pp , A_iTa -collisions, $e^+e^-(\circ)$, $\bar{p}p$, $pp(+)$, $pTa(\bullet)$, $dTa(\square)$, $HeTa(\blacksquare)$, $CTa(\square)$, curve 3.

Fig.6 Total multiplicity distribution of charged secondaries in dTa - collisions at 5.18 AGeV, the curve corresponds to Eq. (1).

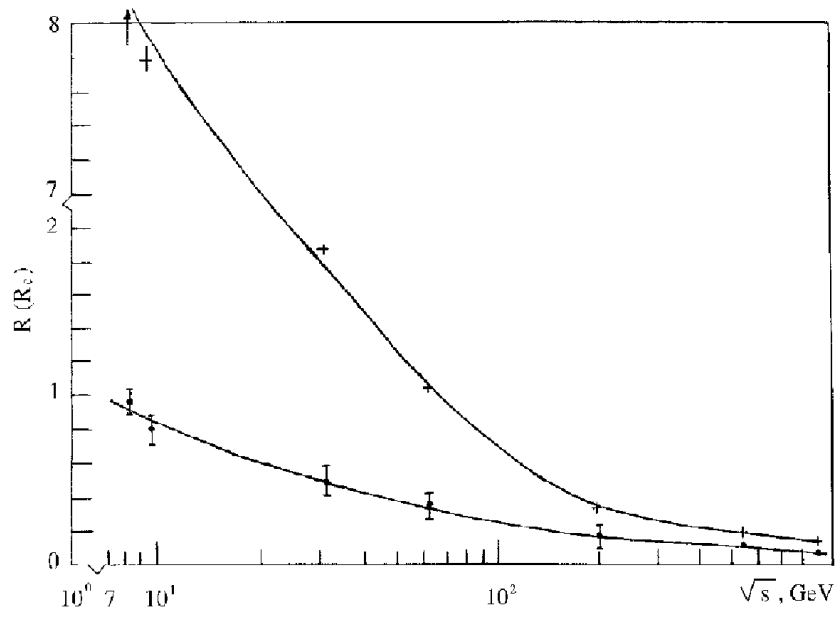


Figure 1:

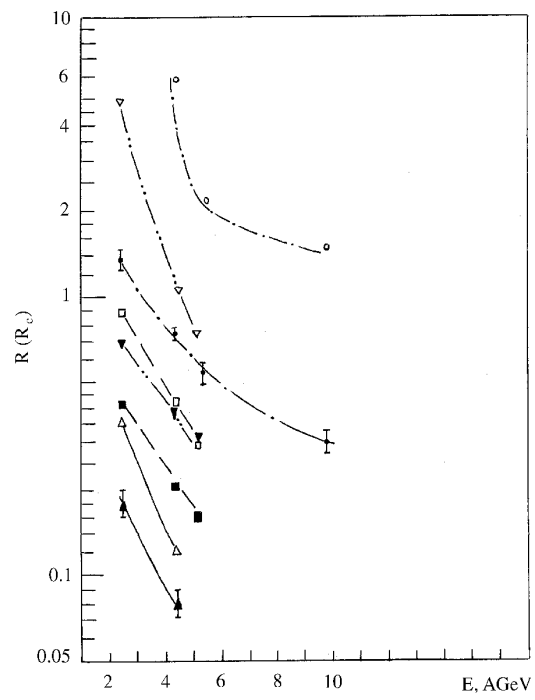


Figure 2:

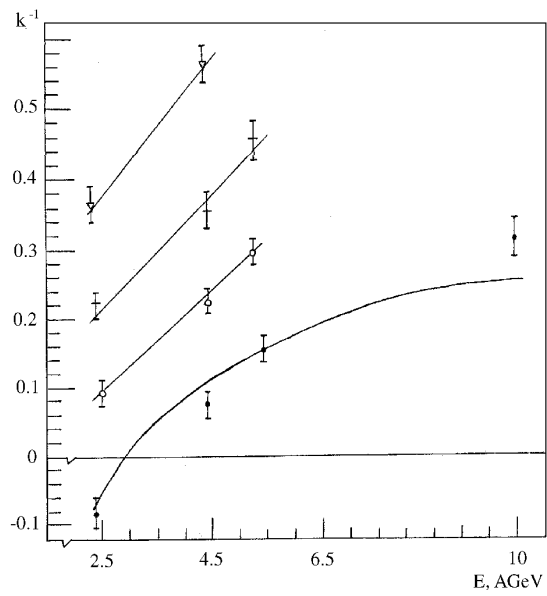


Figure 3:

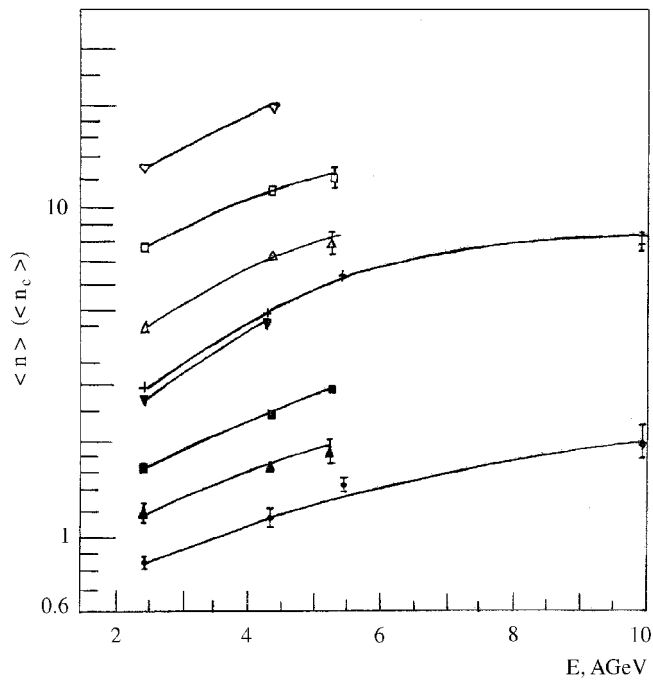


Figure 4:

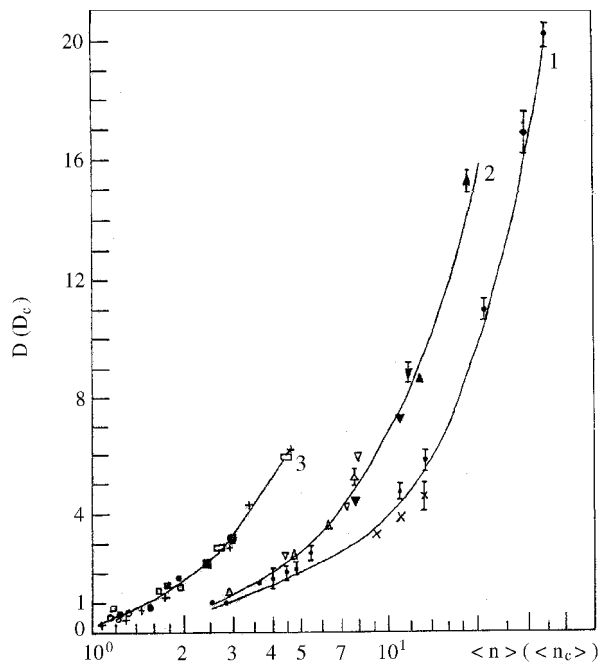


Figure 5:

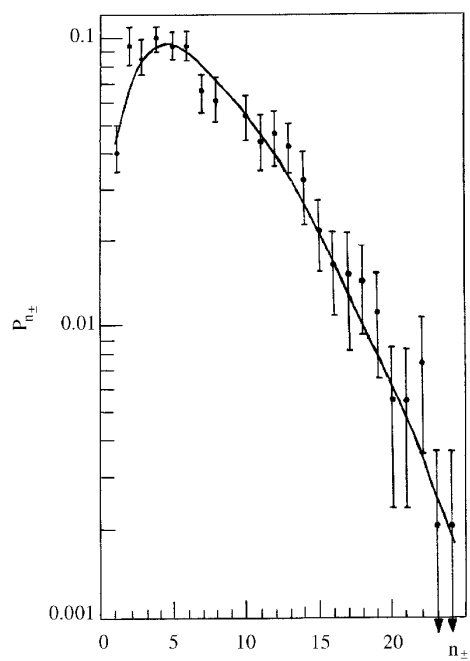


Figure 6: